Received: 4 May 2022 | Revised: 30 June 2022 | Accepted: 6 July 2022

DOI: 10.1002/dvdy.517

Developmental Dynamics WILEY

Gene expression analysis of the *Xenopus laevis* early limb bud proximodistal axis

Daniel T. Hudson[1,3] | **Jessica S. Bromell**[1,4] | **Robert C. Day**[2] | **Tyler McInnes**[1] | **Joanna M. Ward**[1] | **Caroline W. Beck**[1]

[1]Department of Zoology, University of Otago, Dunedin, New Zealand

[2]Department of Biochemistry, University of Otago, Dunedin, New Zealand

[3]Oritain Global, Dunedin, New Zealand

[4]Dairy Goat Co-operative, Hamilton, New Zealand

Correspondence
Caroline W. Beck, University of Otago Ringgold Standard Institution - Zoology, 340 Great King Street, Dunedin 9054, New Zealand.
Email: caroline.beck@otago.ac.nz

Funding information
University of Otago, Grant/Award Number: UORG-Beck-2011

Abstract

Background: Limb buds develop as bilateral outgrowths of the lateral plate mesoderm and are patterned along three axes. Current models of proximal to distal patterning of early amniote limb buds suggest that two signals, a distal organizing signal from the apical epithelial ridge (AER, Fgfs) and an opposing proximal (retinoic acid [RA]) act early on pattern this axis.

Results: Transcriptional analysis of stage 51 *Xenopus laevis* hindlimb buds sectioned along the proximal-distal axis showed that the distal region is distinct from the rest of the limb. Expression of *capn8.3*, a novel calpain, was located in cells immediately flanking the AER. The Wnt antagonist Dkk1 was AER-specific in *Xenopus* limbs. Two transcription factors, *sall1* and *zic5*, were expressed in distal mesenchyme. *Zic5* has no described association with limb development. We also describe expression of two proximal genes, *gata5* and *tnn*, not previously associated with limb development. Differentially expressed genes were associated with Fgf, Wnt, and RA signaling as well as differential cell adhesion and proliferation.

Conclusions: We identify new candidate genes for early proximodistal limb patterning. Our analysis of RA-regulated genes supports a role for transient RA gradients in early limb bud in proximal-to-distal patterning in this anamniote model organism.

KEYWORDS

apical ectodermal ridge, development, distal, limb bud, patterning, proximal, retinoic acid, *Xenopus*

1 | INTRODUCTION

Limb bud development and patterning are best understood in amniotes (recently reviewed in McQueen and Towers 2020[1]). Limbs develop at specific points along the anterior-posterior axis of the embryo, and comprised mesenchymal cells surrounded by an epithelial layer. The mesenchymal cells are derived from lateral plate mesenchyme, and contribute the cartilage, dermis, tendons, and ligaments of the limb.[2] Muscle and nerve cells migrate in from the dermamyotome and spinal cord respectively, and as such are not directly derived from the limb buds.

The early limb bud has three axes which are patterned by signaling centers: proximal-distal, anterior-posterior, and dorsal-ventral. The proximal to distal axis can be seen in the fore- and hindlimb limb skeletal elements of the stylopod (humerus/femur), zeugopod (radius and ulna/tibia and fibula), and autopod (wrist and hand/ankle and foot).

A key player in proximodistal patterning is a region of epithelial cells established at the boundary between dorsal and ventral limb bud surfaces (the future back and palm of the autopod). These cells establish a signaling center, the "apical epithelial ridge" or AER, originally demonstrated by the extirpation experiments of Saunders in chickens. Saunders found that the removal of the AER at 3 days of development resulted in failure of the zeugopod and autopod to form, with the limb truncated at the elbow/knee level. Later AER removal resulted in a failure of just the autopod to form, suggesting that limb skeletal elements are formed in a proximal to distal order.[3] There are two main models for how this patterning is established. The first is the "progress zone" model,[4] which proposes that the mesoderm closest to the AER determines cell fate. As the limb bud elongates, the first cells to leave the progress zone, or the influence of the AER, differentiate into the proximal limb (stylopod), with later cells falling out of range forming progressively more distal elements. An alternative model proposes two signals, Fgfs from the AER antagonizing a proximal retinoic acid (RA) signal.[5] Supporting this "two-signal" model, the Meis homeobox transcription factors Meis1 and 2 are both RA inducible and expressed proximally in developing limb buds.[5] A more recent model, termed "signal-time" has been proposed from grafting experiments in chicken limb buds.[6] This combines an early two signal Fgf/RA model specifying the proximal limb and transition from stylopod to zeugopod, with an intrinsic, timing dependent mechanism taking over to specify the zeugopod to autopod transition and autopod patterning.

Amphibian limb buds develop quite late compared to those of amniotes. *Xenopus laevis* tadpole hindlimbs become capable of autonomous development at stage 48, just as the tadpole begins to feed and when they are still relatively small (reviewed in Keenan and Beck 2015[7]). Fate maps of the hindlimb bud mesenchyme indicate that there is progressive determination of distal skeletal elements as the limb bud grows.[8] Early on, at stages 48 and 49, only the pelvis and femur (stylopod) are determined, the cells destined to form the zeugopod (tibia fibula) first appear distally at stage 50 and the more proximal elements of the autopod (tarsus) at stage 51. Development of the more distal elements depends on the overlying epithelial cells. A morphological AER can be seen in sections from stage 50, but becomes indistinct by stage 53. The biological AER, *fgf8* expression in the innermost layer of the distal epidermis, persists until stage 54 where it associates with growing digits.[9-12] In addition to patterning by distal *fgf8*, we have previously suggested that an opposing and transient RA gradient exists across the stage 51 *Xenopus* limb bud mesenchyme proximodistal axis. From stage 50, *aldh1a2*, the rate limiting step in RA synthesis from vitamin A, is expressed proximally, and *cyp26b*, a catabolic enzyme that degrades RA, is expressed distally in the mesenchyme from stage 51.[13]

In this study, we set out to map differential expression by comparing transcriptomes across three equal proximodistal segments of the stage 51 *Xenopus laevis* hindlimb bud (Figure 1A). In particular, we sought evidence for differential expression of RA-regulated genes across the proximodistal axis, indicative of a transient morphogen gradient at this stage. While the limb bud at stage 51 appears externally featureless, Tschumi's fate maps indicate that the future skeletal elements from pelvis to tarsus are already determined (Figure 1B). However, Tschumi's specification maps show that in the absence of the epidermis, no elements of the autopod develop from grafts of the stage 51 limb bud mesenchyme,[8] supporting the idea that distal elements require signals from the AER in *Xenopus*. The AER with *fgf8* expression is established[9] and mesenchymal RA is expected to be produced proximally and broken down distally.[13] Also in the mesenchyme, cartilage condensation of the future femur is visible histologically, although cartilage marker *sox9* is not yet expressed.[14-16] The distal-most blood vessel, the marginal sinus, which sits right under the AER, is forming at this stage.[14] Nerve invasion into the limb is just beginning proximally[14] and muscle migration has not yet commenced.[17]

Here, we show that genes involved with cell adhesion, cell proliferation, and three signaling pathways: Wnt, Fgf, and RA, are differentially regulated in association with proximodistal position in these early *Xenopus* limb buds. Furthermore, we identify new genes associated with proximal patterning (*tnn.L*, *gata5.L*) and distal epithelium (*capn8.3.L*). Finally, by examining genes previously shown to be regulated by RA in salamander limb regeneration,[18] we identify several RA-regulated genes with clearly graded expression across the proximodistal axis, supporting a role for RA in establishing this axis.

2 | RESULTS AND DISCUSSION

2.1 | Transcriptome analysis of three regions of the early *Xenopus laevis* hindlimb bud proximal to distal axis identified seven clusters of differentially expressed genes

Limb buds at stage 51 were dissected into three equal parts, along the proximodistal axis, and rapidly frozen on

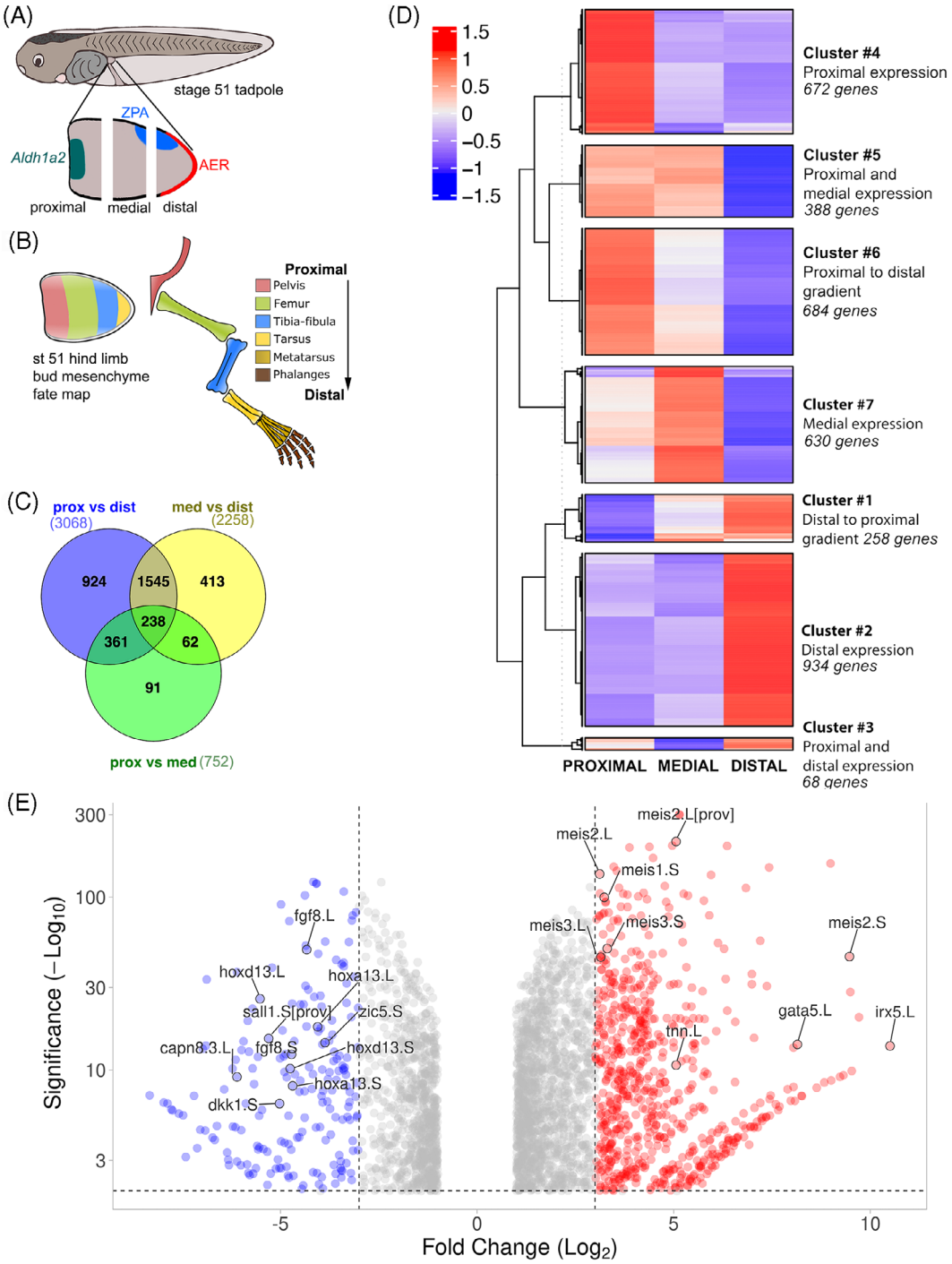

FIGURE 1 Transcriptome analysis of three regions of the early *Xenopus laevis* hindlimb bud proximal to distal axis. (A) Schematic of sample preparation. Stage 51 hindlimb buds were divided into three equal sections along the proximal to distal axis, each part is approximately 200 μM wide. Approximate locations of the apical ectodermal ridge (AER) and zone of polarizing activity (ZPA) are indicated in red and blue, respectively. Location of a potential proximal source of the morphogen retinoic acid is indicated by expression of *Aldh1a2* in green. (B) Fate map showing the contribution of developing stage 51 *X. laevis* hindlimb bud mesenchyme to skeletal elements of the limb, according to Tschumi.[8] (C) Venn diagram of all significantly differentially expressed genes using Venny 2.0.[86] (D) Dendrogram heatmap showing hierarchical clustering of the differentially expressed genes, selecting for seven clusters. (E) Volcano plot showing the relative distributions of known proximal (red: *meis1*, *meis2*) and distal (blue: *fgf8*, *hoxa13*, *hoxd13*) limb genes as well as the genes verified by whole mount in situ hybridization in Figures 2-4). Genes with log2 fold change <3 in either direction are represented by grey dots

dry ice before extracting RNA. The approximate locations of the cuts are shown in Figure 1A, with each segment measuring approximately 200 μm along the proximal-distal axis, 400 μm across the anterior-posterior axis, and 200 μm along the dorsal-ventral axis. These dissections are not expected to neatly divide the limb bud into future

stylopod, zeugopod, and autopod. Compared to the mesodermal fate map for this stage, the future autopod and some of the zeugopod would be derived from the distal segment, pelvis and some stylopod from the proximal segment, and stylopod/zeugopod from the medial part[8] (Figure 1B). The AER is expected to be exclusively captured in distal sections, with the ZPA split between distal and medial sections. Regression analysis of mapped transcriptome read counts showed that replicate samples clustered closely together ($r = .98$, .99, and 1.00 for proximal, medial, and distal respectively). Pearson correlations of read count means showed that proximal and medial stage 51 limb bud transcriptomes are more similar to each other ($r = .97$) than to distal ($r = .80$ to proximal and $r = .65$ to medial).

Differentially expressed genes were defined as genes with normalized read counts >log2 fold change ± 1 or higher, and with a P value < .05, between any two limb bud regions (Figure 1C,D), which captured a total of 3682 genes. As expected, the number of differentially expressed genes between proximal and distal was highest (Figure 1C). Clustering of the 3682 differentially expressed genes into seven clusters best represented the patterns expected across developing limbs (Figure 1D). Cluster 2 is the largest group, containing 934 genes with predominantly distal location, including both homeologs of the AER marker *fgf8*, the ZPA morphogen *shh.L* and distal mesenchyme markers *hoxd13* and *hoxa13*. Cluster 4 contains 672 proximally located genes, including established proximal limb markers *meis1* and *meis2*. More graded expression is seen by genes in clusters 6 (highest proximal, 684 genes) and 1 (highest distal, 258 genes). Cluster 5 has genes that are high in proximal and medial but low distal (388 genes). Cluster 3 is the smallest, with genes that are predominantly expressed in the distal and proximal regions but not the medial (68 genes), and cluster 7 genes are opposite, with highest levels in the medial limb bud (630 genes).

2.2 | Genes expressed in the proximal limb bud include *gata5.L*, *irx5.L*, and *tnn.L*

Figure 1E shows the most proximal (red circles) genes, taking account of both fold change and significance, generated from the proximal versus distal reads. Many of these genes are found in cluster 4 (Figure 1D), which groups 672 genes with much higher expression in the proximal limb bud than in either medial or distal sections. This group includes *aldh1a2.L* (formerly known as *raldh2*, previously shown to be proximally expressed by us[13]). It also includes several family members of the Meis homeobox transcription factors (*meis3.L*, *meis3.S*, *meis2.S*, *meis2.L*, *meis1.S*). *Meis1* and *Meis2* are proximal genes with a well-established functional role in limb patterning in amniotes[19] but *Meis3* has not been previously associated with limb development.

Three almost exclusively proximal genes found in Cluster 4 were verified using whole mount in situ hybridization: *gata5.L*, *irx5.L*, and *tnn.L* (Figure 2). *Gata5* encodes a zinc finger transcription factor associated with heart and liver development in *Xenopus*[20] and has not been previously associated with limb development. *Gata5* reads were almost exclusively in the proximal limb transcriptome (Proximal > Distal Log2 FC 8.1 and 8.0 for L and S forms respectively), and whole mount in situ hybridization confirmed a faint but very localized basal spot of *gata5.L* expression in stage 50 and 51 limb buds, which became clearer at stage 52 (Figure 2A-C). The related transcription factor Gata6 regulates shh in anterior mouse limb development.[21,22] However, this does not fit with the central basal location of *gata5.L* in frogs. *Gata5.L* in embryos (data not shown) showed clear expression in the heart as previously reported.[23]

Irx5 encodes a homeobox transcription factor of the Iroquois family. Both L and S forms are expressed at much higher levels in proximal than in distal or medial limb segments, (P > D Log2 FC 10.5 for *irx5.L* and 6.8 for *irx5.S*). *Irx5.L* was the most over-represented proximal gene and in situ hybridization for *irx5.L* confirmed this distribution, with expression basal, proximal and increasingly anteriorly localized in hindlimb buds from stage 50 to 52 (Figure 2D-F). Embryonic expression of *irx5.L* in the brain and eye (data not shown) matched that of previous reports,[24] although at this stage the *S* homeolog has the strongest expression.[25] *Irx5* has been previously associated with limb patterning in mammals, where it has shown it to be functionally redundant with *irx3*. Mouse double *irx3/5* knockouts have a reduced femur and are missing the tibia and digit 1,[26] showing that these genes are important for both proximal and anterior limb development. *Irx3.L* and *S* genes show similar expression profiles to *irx5*, with P > D log2 fold change 4.8 for the L form and 6.8 for the S form, suggesting that they may also act together in *Xenopus* limb patterning. In humans, Hamamy syndrome (OMIM 611174, *IRX5*[27]) has no reported limb defect, possibly due to compensation by *IRX3*.

Tenascins are extracellular matrix glycoproteins, and *Xenopus laevis* has a single copy of Tenascin N (*tnn.L*) which is expressed most strongly in the proximal third of the limb bud at stage 51, with almost no read counts in the medial or distal segments (Proximal > Distal Log2 fold change 5.1). Tenascin N was originally identified in

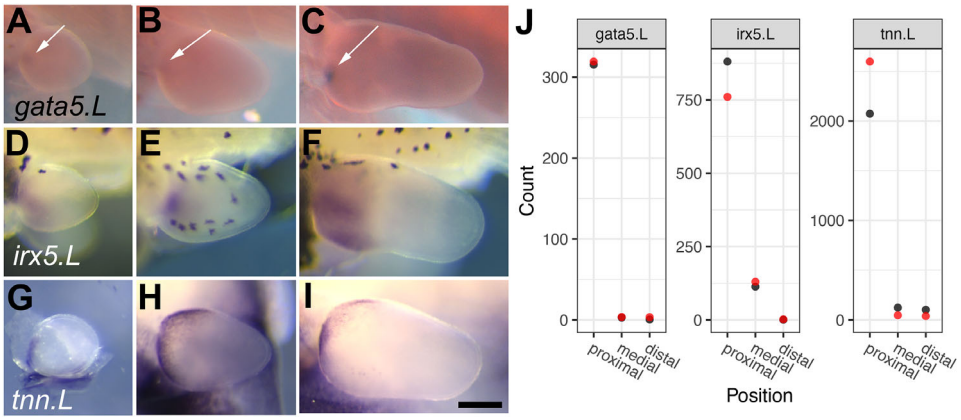

FIGURE 2 Expression of three cluster 4 proximal genes in *X. laevis* hind limb buds. (A-I) Whole mount in situ hybridization (purple staining) of stages 50 to 52 hind limb buds as viewed from the dorsal side, posterior uppermost. (A-C) white arrows indicate proximal spot of mesenchymal *gata5.L* at stage 50 (A), 51 (B), and 52 (C). (D-F) *irx5.L* in the proximal mesenchyme at stage 50 (D), 51 (E), and 52 (F). Black stellate cells are melanophores in nonalbino tadpoles (D-F), expression in stage 52 is anterior as well as proximal. (G-I) Expression of *tnn.L* is very strong along the boundary with the body wall, and is epithelial. Stage 50 limb bud dissected to enable visualization of limb bud, as there is strong expression in the ventral fin as well as the limb bud (G), stage 51 (H), and 52 (I). Scale bar in (I) is 250 μM and applies to all panels. (J), Normalized read counts of *gata5.L*, *irx5.L* and *tnn.L* in the three sections of the stage 51 limb bud transcriptome. Red and black dots indicate biological replicate data, where only red can be seen it overlaps completely with black

zebrafish[28] and is more commonly known as Tenascin-W. It is a chordate-specific gene with no known links to limb development.[29] *Tnn.L* expression was confirmed as proximal in stage 50 to 52 limb buds (Figure 2G-I) where it appeared to be epithelial, expressed where the limb bud meets the trunk. Expression persists in older limbs but the proximal localization is lost (data not shown). In tailbud stage embryos, *tnn.L* was expressed only in the anatomical tail bud (data not shown).

2.3 | Genes expressed in the distal limb bud

Distally expressed genes, with much lower levels of expression in either medial or proximal limb bud thirds are found in cluster 2, which contains 934 genes (Figure 1D). *Fgf8*, *bmp4*, *dlx2*, *dlx3*, and *sp8* all have localized expression in the developing AER of mouse limbs.[30-33] Neither *bmp4.L* nor *S* were differentially expressed in *Xenopus* stage 51 hindlimbs, but *fgf8.S*, *fgf8.L*, *sp8.L*, and *sp8.S* and the distal-less homeobox genes, *dlx2.S*, *dlx2.L*, *dlx3.S*, and *dlx3.L*, as well as the S homeolog of *dlx4*, were all cluster 2 genes. *Bmp2.S* and *bmp7.1.L* also appear in this cluster.

Three genes chosen for their almost exclusive expression in the distal stage 51 limb bud were confirmed as being located exclusively in the distal epithelium (Figure 3). Their distribution was highly significantly enriched in distal stage 51 limb bud, similar to that of the AER specific gene *fgf8* (Figure 1E). *Capn8.3.L* (D > P Log2 fold change 6.2, cluster 2) encodes a calcium dependent cysteine protease (calpain). Whole mount in situ hybridization revealed *capn8.3.L* expression in the region of the forming AER at stage 50 and 51, with expression margins becoming very defined at stage 52 and maintained in the distal epithelium of the forming digits until stage 55 at least (Figure 3A-E).

Closer scrutiny showed that the AER margin cells do not express *Capn8.3.L*, but rather it is expressed either side of the boundary, and appears stronger on the dorsal side. (Figure 3F,G). *Capn8* is considered a classical calpain and *capn8* is expressed in the gastrointestinal tract of mammals (reviewed in Spinozzi et al.[34]). In *Xenopus*, it was identified as a downstream target of Tfap2, expressed throughout the non-neural ectoderm in neurula stage embryos,[35] so it may have a role in boundary definition. *Capn* genes have not been previously associated with vertebrate limb development. *Capn8* likely originated in the ancestor of jawed vertebrates[36] where it may have assumed a role in neural crest before being later co-opted into limb development. In *X. laevis*, *capn8* appears to have been duplicated many times: *capn8.1*, *8.2*, *8.3*, *8.4*, and *8.5* are clustered together with *capn2.L* on the 5L chromosome and *capn8.1* and *8.6* cluster with *capn2.S* on the 5S chromosome (data from *X. laevis* genome build v9.2 on Xenbase[37]). In the diploid *X. tropicalis*, *capn8.1*, *8.2*, *8.3*, *8.5*, and *8.6* are clustered together with *capn2* on chromosome 5. *Capn8.2.L* was also a cluster 2 gene, mainly expressed in distal hindlimb samples, albeit at lower levels than *capn8.3L*, suggesting that they could be co-regulated.

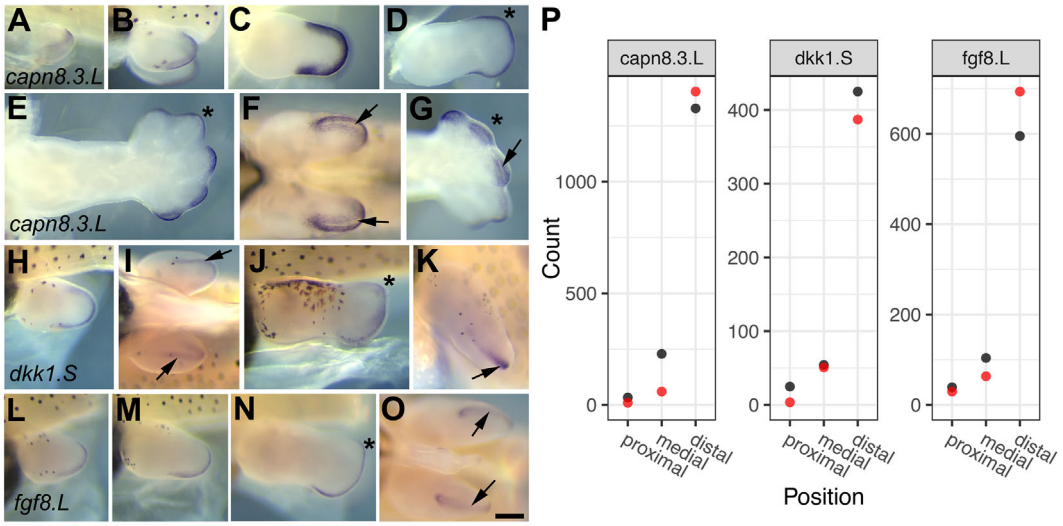

FIGURE 3 Expression of distal epithelial genes in *X. laevis* hindlimb buds. (A-O) Whole mount in situ hybridization, gene expression is marked by dark purple staining. (A-G) *Capn8.3L* is expressed in the epithelial cells flanking the AER. (A-E) Dorsal view of limb with distal to the right and posterior uppermost. (A): stage 50, (B): stage 51, (C): stage 52, (D): stage 53, (E): stage 55. (F and G) Views of the distal limb(s) to show the AER (black arrow), (F): stage 53, (G): stage 55. (H-K) Expression of *dkk1.S* (H): stage 51, dorsal view, (I): distal view, (J): stage 53 dorsal view, (K): distal view. (L-O) expression of *fgf8* (L): stage 51 dorsal view, (M) stage 52 dorsal view, (N): stage 53 dorsal view, (O): stage 53 distal view. Black arrows indicate the AER in distal views, and the approximate position of digit IV is indicated by an asterisk from stage 53. Black stellate cells are melanophores in non-albino tadpoles (B, H-M). Scale bar in (O) is 250 μM and applies to all panels. (P) Normalized read counts of *capn8.3.L*, *dkk.S* and *fgf.S* in the three sections of the stage 51 limb bud transcriptome, red and black indicate biological replicate data

Both homeologs of *dkk1* were cluster 2 genes. *Dkk1.S* (distal > proximal Log2 fold change 5.0), encodes dickkopf 1, an extracellular Wnt signaling antagonist that acts upstream of receptor activation. *Dkk1* was first discovered in *Xenopus*[38] and is one of three dickkopf genes. In *Xenopus* hindlimbs, *dkk1* expression is AER-specific from stage 51 (Figure 3H-K). Expression mimics that of *fgf8*, in the AER (Figure 3L-O). This is very different from *dkk1* expression in the mouse limb bud, which is mesenchymal, and at the equivalent stage is expressed in two proximal spots, one posterior and slightly overlapping *shh* (ZPA) and one anterior,[39,40] with later expression is in the interdigits. *Dkk1* knockout mice are non-viable and have fused and duplicated digits resulting from an expanded AER.[41] In chickens, overexpression of *dkk1* leads to apoptosis of the AER cells and subsequent limb truncation.[42] While this clear difference in expression of *dkk1* in limb buds of amniotes (mesenchyme) and *Xenopus* (AER) is unexpected, a search for *dkk1* enhancers identified a conserved element in the 3′ UTR which was able to drive expression of a reporter very specifically in the developing mouse limb bud AER.[43] This element is conserved in fish, and therefore could also be present in *Xenopus*. Conversely, perhaps the mesodermal enhancer has been lost or masked in frogs.

The role of the fibroblast growth factor member Fgf8 in AER function and limb outgrowth in amniotes is well established[44,45] and the expression of *fgf8* in the AER has also been well documented in *Xenopus*[9,10,12] Both *fgf8* homeologs were in cluster 2 and *Fgf8.L* (distal > proximal Log2 fold change 4.3) is shown here for comparison (Figure 3L-O).

2.3.1 | *Zic5.S* and *Sall1.S* are expressed in the distal limb bud mesenchyme

Cluster 2 also contains several genes known to be preferentially expressed in the distal mesenchyme of amniote limb buds, including both homeologs of *fgf10*. Also in cluster 2 are 5′ hox transcription factors *hoxa13.S*, *hoxa13.L*, *hoxd13.S*, and *hoxd13.L* (Figure 1E), previously shown to be distally expressed in *Xenopus* hindlimbs.[46] Genes coding for several family members of the receptor tyrosine kinase/Fgf antagonist Sprouty (Spry) are also found in cluster 2 (*spry4.L*, *spry4.S*, *spry1.L*, *spry1.S*, and *spry2.L*). We have previously shown that *X. laevis spry2* was expressed in limb bud AERs, and *spry1* and *spry 4* in limb bud mesenchyme.[12]

Two genes encoding transcription factors found in with cluster 2 that were highly significantly enriched in distal stage 51 limb bud (Figure 1E) were validated and further analyzed using whole mount in situ hybridization

of *Xenopus* hindlimbs. Mutations in the gene coding for the spalt-like zinc finger transcription factor Sall1 are associated with Townes-Brocks syndrome (OMIM #107480). The phenotype includes extra thumbs, radial dysplasia and foot deformities[47] which suggests a role in anterior-posterior limb axis patterning of the autopod and zeugopod. *Sall1* is expressed in stage E10.5 mouse limb buds and has a distal mesenchyme and AER expression pattern in early chicken limb buds.[48,49] *Sall1.S* reads were almost exclusively found in the distal hindlimb samples (distal > proximal log2 fold change 5.3). Expression of *sall1.S* was localized to the distal mesenchyme at stage 50 and 51 (Figure 4A,B,E), but from stage 52 the expression was lost from the most distal cells, and was stronger anteriorly and dorsally (Figure 4C,D,F). *Xenopus* has four *spalt*-like orthologous: *sall1.L*, *sall3.L*, and *sall3.S* were also cluster 2 genes, *sall4.L* and *sall4.S* were found in cluster 1. Previous work by Neff et al revealed the role of *sall4* in *Xenopus* limb regeneration, and stage 53 control limbs appear to have similar expression to *sall1* here.[50] *Sall2* homeologs were not represented in any of the clusters, and read numbers were very low suggesting *Sall2* is not a key player in limb developmental patterning in early *Xenopus* limbs.

The zic family of zinc finger transcription factors are orthologous of *Drosophila odd-paired*, with tetrapods, including *Xenopus*, normally have five family members.[51,52] Cluster 2 contains several distally located *zic* genes (*zic1.S*, *zic2.L*, *zic2.S*, *zic3.L*, *zic3.S*, *zic5.L*, and *zic5.S*). *Zic1* and *zic4* form a tandem pair on chromosomes 5S and 5L, homeologs have very few, mostly distal reads in limb buds. *Zic3* is a singleton in tetrapods, and is expressed distally, and *zic2* and *zic5* form a tandem pair on chromosomes 2S and 2L, and have much higher read counts. *Zic2* has been previously shown to be expressed in distal limb bud mesenchyme in mice,[53] but *zic5* has no known association with limb development. *Zic5.S* (distal > proximal log2 fold change 3.9) expression was validated using whole mount limb in situ hybridization (Figure 4G-L). Expression was seen very faintly in distal mesenchyme at stage 51 (Figure 4G,K) and in two regions at stage 52, a broad expression in the distal anterior and a more restricted stripe in posterior mesoderm (Figure 4H). After stage 52, the expression in posterior mesenchyme was lost, with anterior/dorsal expression maintained in the forming autopod at stage 53 to 54 (Figure 4I,J,L).

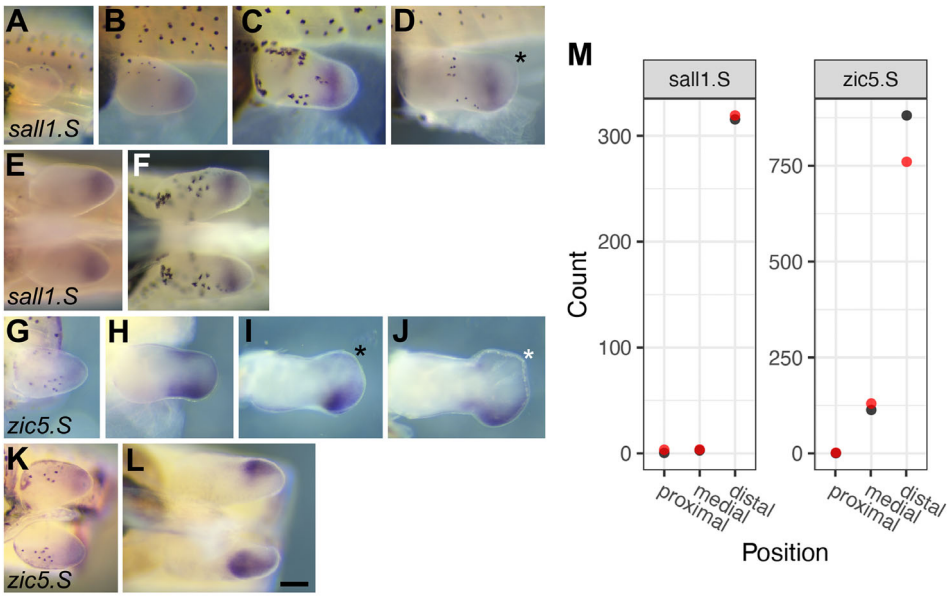

FIGURE 4 Expression of two distal mesenchymal genes in *X. laevis* hindlimb buds. (A-L) Whole mount in situ hybridization where expression is indicated by dark purple staining. (A-F) expression of *sall1.S*. (A-D) Dorsal views of the limb with distal to the right and posterior uppermost. (A): stage 50, (B): stage 51, (C): stage 52, (D): stage 53. (E and F) Views of the distal limb, the ventral midline of the tadpole running left to right in the center of the image. (G-L) Expression of zic5.S indicated by dark purple staining. (G-J) Dorsal views of the limb. (G): stage 51, (H): stage 52, (I): stage 53, (J): stage 54. (K and L) Views of the distal limb, (K): stage 51, (L) stage 54. Asterisk indicates the approximate location of digit IV in stage 53 and above limb buds. Melanophores are present on some limb buds (A-D, F, G, and K) as black stellate cells. Scale bar in (L) is 250 μM and applies to all panels. (M) Normalized read counts of *sall1.S and zic5.S* in the three sections of the stage 51 limb bud transcriptome, red and black indicate biological replicate data, where only red can be seen it overlaps completely with black

2.4 | Genes with differential expression across the proximodistal axis were associated with cell adhesion, cell proliferation, as well as Wnt, Fgf, and retinoic acid signaling

We annotated 894 genes with differential expression of log fold change ± >1.5 between proximal and distal limb bud samples, and analyzed these for over-represented gene ontologies at all levels, compared to all *X. laevis* annotated genes (9414). The complete data for 36 over-represented GO terms, at all levels, can be found in the Appendix S1, but we will highlight the most pertinent ones here.

2.4.1 | Cell adhesion

Differential cell adhesion has been shown to correlate with proximodistal position in early limb buds.[54] In the *Xenopus* stage 51 hindlimb, 56 genes with differential proximodistal expression were associated with the GO term "cell adhesion". Nineteen of these had significantly more reads in the distal third and 34 had more in the proximal third (three genes were removed due to having low read numbers; Figure 5). Of particular interest is *Agr2.L*, which codes for a thioredoxin domain, secreted, GPI anchored cell surface protein. Agr2 was originally identified as nAG (newt anterior gradient), which is a ligand for the salamander Prod1 receptor, which plays a role in establishing proximodistal identity in limb regeneration.[55]

Additionally, we identified proximodistal differential expression of genes encoding members of the integrin, cadherin, thrombospondin, and nidogen families. Six genes encoding integrins, which mediate cell to matrix adhesion, were differentially expressed, with those coding for subunits α8, α11, and α2b found at highest levels in the proximal limb bud and α4, β6, and β7 found at highest levels distally. Cadherins (Cdh) are calcium-dependent transmembrane molecules involved in cell to cell adhesion. *Cdh20* was almost exclusively expressed distally, whereas *cdh2* (N-cadherin), *cdh6*, *cdh13*, *cdh15*, and *19* were highest in the proximal segment. The cadherin-related desmoglein *dsg2* is found proximally. Protocadherins *pcdh19* and *17* are distal, whereas *pcdhgc5* is proximal.

Thrombospondins (*Thbs1-4*) are calcium binding, extracellular matrix proteins implicated in skin wound healing in mammals. In *X. laevis* limb buds, *Thbs3* and *4* are distal (cluster 2) and *Thbs2* is proximal (cluster 6S/4L). Thrombospondins have been previously implicated in axolotl limb development and regeneration[56] and *X. laevis* limb regeneration.[57] The basement membrane protein Nidogen (Ndg) has two members, *ndg1* is proximal, whereas *ndg2* is distal. In mice, the two nidogens appear redundant, but double knockouts have soft tissue syndactyly resulting from failed interdigital apoptosis.[58]

2.4.2 | Wnt agonists and antagonists are both proximally and distally expressed

The Wnt signaling pathway is most often associated with dorsal-ventral limb patterning, especially the ligand Wnt7a, which helps establish the position of the AER at the dorsal ventral boundary and restricts *lmx1b* to dorsal mesenchyme.[59] Here, we found Wnt pathway genes were significantly over-represented in our proximal-distal analysis. *Dkk1.L* and *.S*, which code for Wnt pathway antagonists, were the most distally biased genes in this set, are captured in cluster 2, and the AER-specific expression of *dkk1.S* has been previously discussed (Figure 3). Interestingly, *Dkk2.S* shows the opposite polarity, with over 80% of transcripts on the proximal limb bud. In *Xenopus* embryos, Dkk2 acts as an activator of canonical Wnt signaling rather than an antagonist[60]: so both expression and function of these two *dkk* genes are in opposition. *Dkk2.S* is a cluster 4 gene, but its homeolog *dkk2.L* falls into cluster 7, as does another family member, *dkk.3.S*. Cluster 7 genes have highest expression in the medial limb bud, which would indicate that there is a Dkk associated with each of the three proximodistal domains in *Xenopus* limbs. Interestingly in mice, *dkk1*, 2, and 3 are all mesenchymal in developing limb buds, with complementary expression patterns around the time of mesodermal condensation formation.[40] *Xenopus* Dkk3 does not appear to modulate Wnt signaling[60] and instead affects mesoderm induction via interference with TGFβ pathways.[61]

Genes encoding the ligands Wnt4, 16, and 11 are more proximal and Wnt10a, 11b, and 5a are more distal. Wnt5a is associated with some cases of autosomal dominant Robinow syndrome, a rare form of dwarfism with shortening of the mid and distal parts of the limbs. It is expressed in the mesoderm just under the AER, often referred to as the progress zone, in chicken limb buds.[62] The same expression is seen in axolotl and mouse limb buds, and *wnt5a* null mice have distally truncated limbs.[63,64] The effect of Wnt5a on limb proximodistal patterning is mediated through the planar cell polarity pathway rather than canonical Wnt signaling and is dependent on AER Fgf signals.[65] Notum is a Wnt pathway antagonist, with expression highest in the distal limb bud. Expression in the early chicken limb was previously shown to be mainly in the AER.[66] In contrast, secreted frizzled related protein genes, encoding antagonists known as Sfrps, are predominantly expressed in the medial and proximal limb bud. Sfrp are able to antagonize Wnt by mimicking receptors and binding Wnt, but

may also have other non-Wnt roles (for review see Nathan et al.[67]).

2.4.3 | Cell proliferation and response to fibroblast growth factor

FGF pathway agonists and antagonists are both proximally and distally expressed in stage 51 *Xenopus* hind limb. The role of AER-Fgf signaling in proximodistal vertebrate limb bud patterning is well established, with Fgf8 as the key functional molecule.[44,45] We have already discussed *fgf8* (Figure 3). Amniotes have additional Fgfs in the AER, such as Fgf4, 9, and 17.[68] *Fgf4* transcripts were not detected in *Xenopus* hindlimb buds at stage 51, however, *fgf9*, *fgf10*, and *fgf16* are additional distal Fgfs (all in cluster 2). Conversely, *fgf7* is proximal, S/L forms are found in cluster 6/4, respectively.

Most of the genes associated with the GO term cell proliferation are located predominantly in the distal limb,

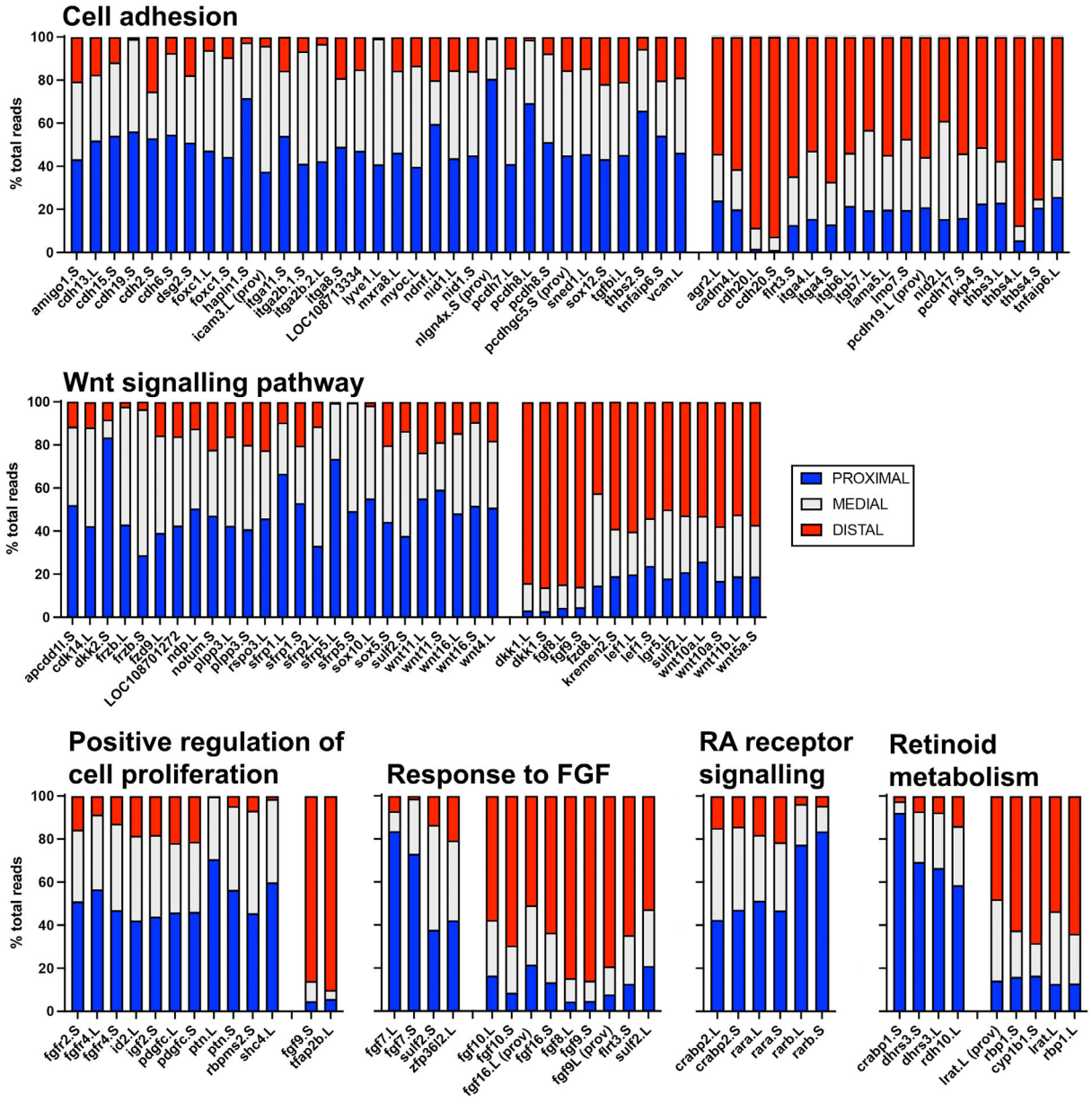

FIGURE 5 Relative distribution of read counts for genes in differentially expressed gene ontology gene sets for cell adhesion, Wnt signaling pathway, positive regulation of cell population proliferation, response to fibroblast growth factor, retinoic acid receptor signaling, and retinoid metabolism. Stacked graphs show the percentage of proximal reads is in blue, medial reads in grey, and distal in red. Genes with statistically more reads in distal than proximal are on the left and those more proximal on the right, and are ordered alphabetically within each group.

including transcripts for growth factors Igf2 and Pdgfc, and Fgf receptor coding genes *fgfr2* and *fgfr4*. The remaining two Fgf receptor genes are expressed at similar levels in all three proximodistal regions of the stage 51 limb bud (Appendix S1). Over 90% of transcripts for cluster 2 genes *tfap2b* and *fgf9* are in the distal limb. Oddly, the two *X. laevis* homeologs of *sulf2*, encoding heparan sulfate 6-O-endosulfatase enzymes, are expressed in different regions, with the S-form proximal and the L-form distal, as previously confirmed by in situ hybridisation.[69] Sulf2 was also captured in the Wnt signaling GO.

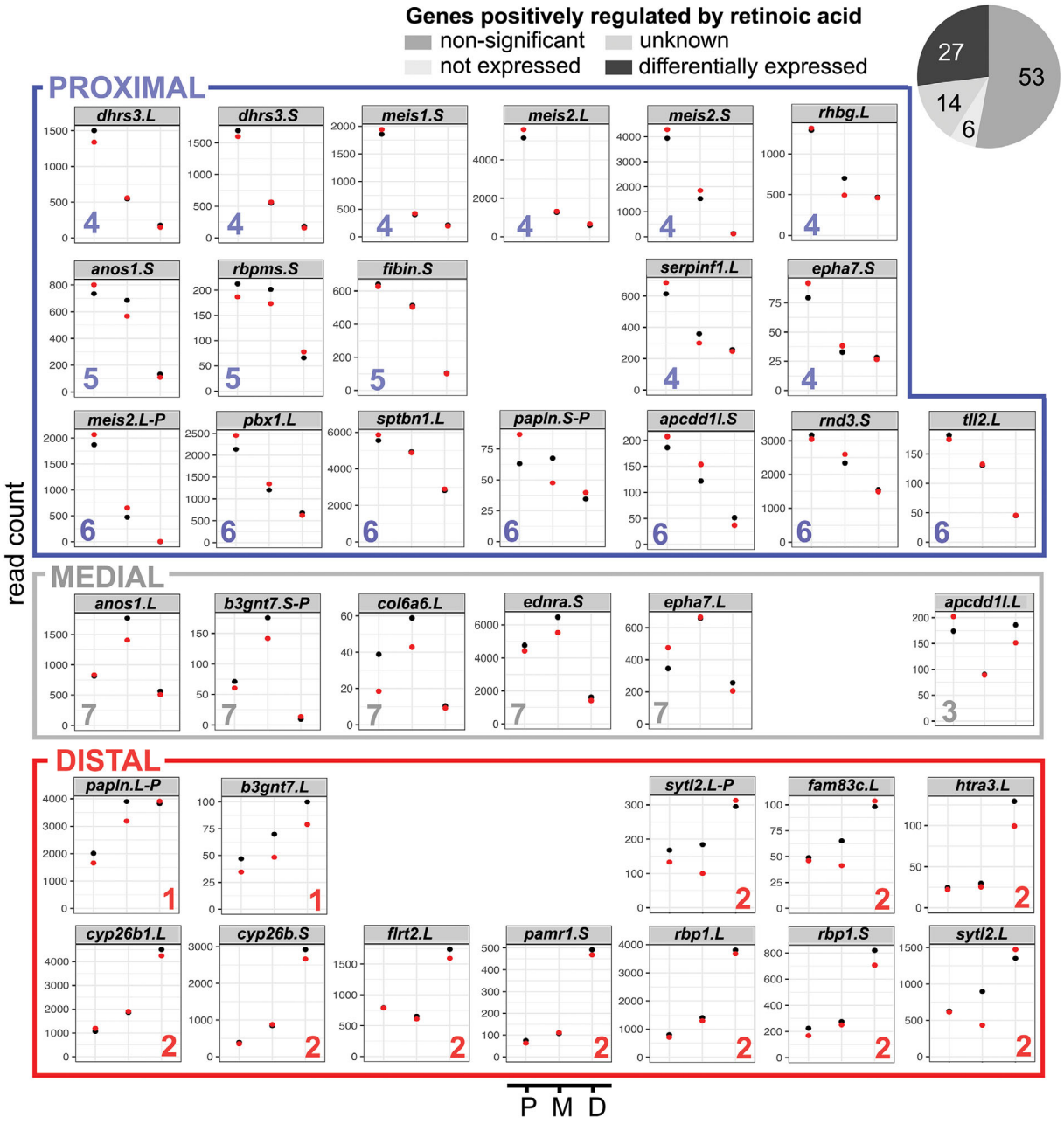

FIGURE 6 Genes previously shown to be upregulated by retinoic acid in axolotl limbs do not show consistent expression distributions in *Xenopus* limbs. One hundred different genes identified as upregulated by RA in axolotl limb[18] were identified one of four categories: unknown (no *Xenopus* homologue), not expressed (not found in *Xenopus* stage 51 limb bud), nonsignificant (expression is not significantly different across the three limb bud sections) or differentially expressed. Homologs of the 27 differentially expressed genes in the allotetraploid *Xenopus laevis* are found in all seven clusters, cluster number is indicated by colored number at the base of each graph, read counts are shown on the *y*-axis and position on the *x*-axis. P = proximal, M = medial, D = distal. Replicates are represented by red and black dots and where only one dot can be seen, these overlap completely. Colored boxes are used to group clusters with proximal, distal or medial/terminal expression patterns

2.4.4 | Retinoic acid metabolism and signaling

RA is proposed as a proximal signal opposing distal Fgf to establish expression domains across forming limb buds.[5] Two GO terms associated with RA were found to be significantly associated with proximal versus distal gene expression in our stage 51 hindlimbs (Figure 5). RA receptor signaling genes were all proximally biased, and included the genes for retinoic acid receptor subunits A and B (*rara*, *rarb*), and the binding protein Crabp2 (previously characterized in McEwan et al[13]). *Rarb* showed particularly strong proximal bias, and a third RA receptor-encoding gene, *Rarg* was not differentially expressed (Appendix S1). Genes associated with retinoid metabolism were also over-represented, with both proximal and distally biased expression (Figure 5).

2.5 | Retinoic acid downregulated genes are expressed in the distal hindlimb segment

RA has been demonstrated to reprogram distal cells to a more proximal fate in chicken limb bud grafts,[70] and exposure to RA in regenerating frog limb buds[71] and axolotl limbs[72] results in proximodistal duplications, suggesting RA disrupts pattern along this axis. RA is produced endogenously from vitamin A and can modulate genetranscription via binding to RA nuclear receptors that recognize RA response elements (RARES) in enhancers.[73] RA reporter activity has been detected in forelimbs, but not hindlimbs, during axolotl development.[72] We previously showed the presence of opposing RA synthesis and catabolic genes in early developing *Xenopus* limb buds. To see if there was any evidence from RA target genes to support a functional

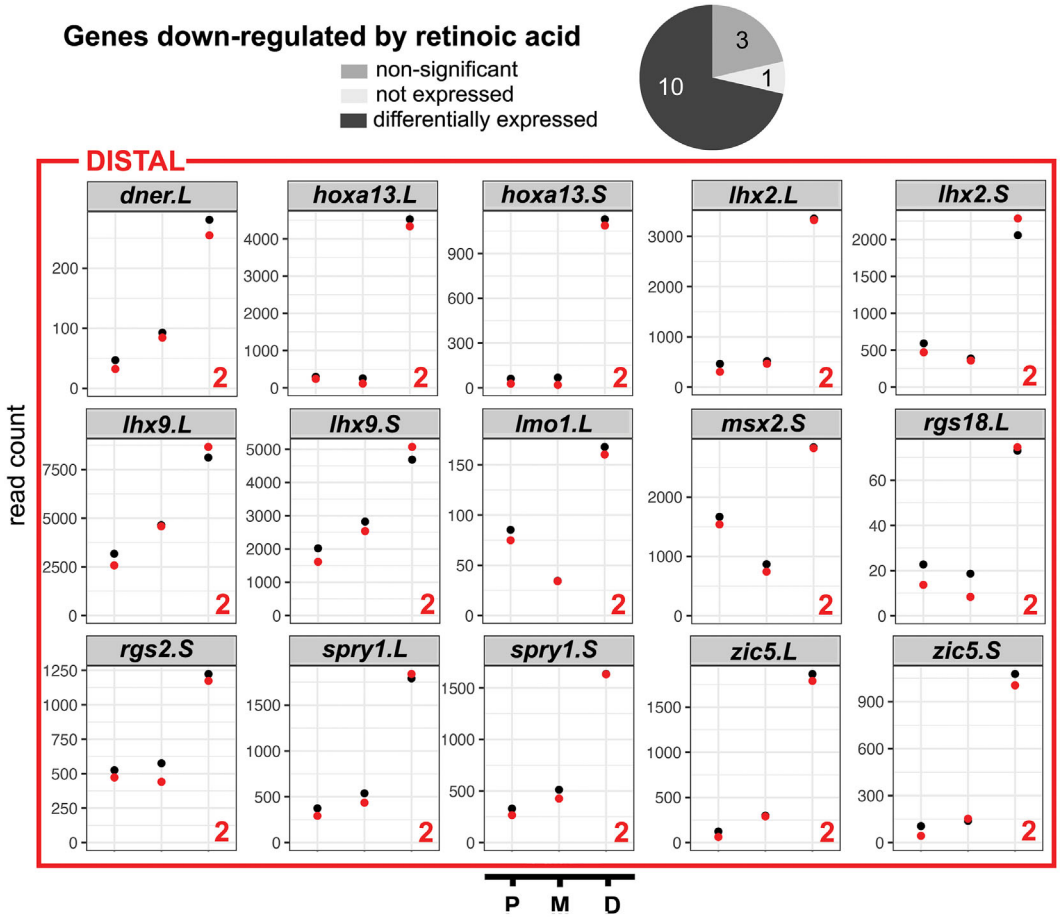

FIGURE 7 Distal gene expression in stage 51 *Xenopus* hindlimb bud of genes previously shown to be downregulated by retinoic acid in axolotls. Pie chart: 14 different genes identified as downregulated by RA in axolotls[18] were identified as not expressed (not found in *Xenopus* stage 51 limb bud), nonsignificant (expression is not significantly different across the three limb bud sections) or differentially expressed. Homologs of the 10 differentially expressed genes in the allotetraploid *Xenopus laevis* are found exclusively in cluster 2. Cluster number is indicated by colored number at the base of each graph, read counts are shown on the *y*-axis and position on the *x*-axis. Replicates are represented by red and black dots and where only one dot can be seen, these overlap completely. P = proximal, M = medial, D = distal. Colored box indicates all genes had distal expression patterns

role for RA gradients in the early limb bud, we looked at the proximodistal distribution in *Xenopus* stage 51 hindlimb of genes identified as upregulated or downregulated by RA treatment in a prior study of axolotl limb regeneration.[18] Nyugen et al identified 101 genes as upregulated by RA, 14% of these had no recognized homologues. Of the remaining genes, 62% were not significantly differentially expressed across *Xenopus* stage 51 limb buds, and a further 7% were not expressed in limb buds at all. Twenty-seven genes (31%) were differentially expressed (Figure 6) with all clusters represented. Proximally expressed genes were most common (18 genes, clusters 4, 5, and 6) followed by distal genes (13 genes, clusters 1 and 2) and 5 genes were predominantly expressed in the medial region (cluster 7) with one gene lowest in the medial region (cluster 1). Therefore, although many salamander RA upregulated genes had differential expression across the proximodistal axis in stage 51 frog hindlimb buds, there was no consistent pattern observed. However, *meis* genes were consistently found in cluster 4 (proximal genes), as expected from previous work,[5] and the related homeobox gene Pbx1 was in cluster 6 (proximal to distal gradient). Our findings of proximal-biased expression for these genes therefore support the role of Meis homeobox transcription factors as RA-regulated mediators of proximal identity. The finding that conditional inactivation of *meis1/2* in mice results limb phocomelia, where proximal elements were missing but distal ones develop normally, further demonstrates the importance of RA-regulated genes in limb proximodistal patterning.[19]

As well as promoting the proximal to distal spatial pattern via upregulation of Meis homeobox proteins, it is possible that RA might also play a role in limiting the expression of distally localized genes via inhibition. Interestingly, of the 14 genes identified in axolotl limb regeneration as downregulated by RA,[18] ten (72%) were differentially expressed across the early *Xenopus* limb buds with all of these falling into cluster 2 indicating predominantly distal expression (Figure 7). A further three genes were present in limbs but not differentially expressed, and one gene was not expressed in limb buds. While distal expression is indicated by inclusion in cluster 2, *hoxa13*, *lhx2*, *rgs18*, *rgs2*, *spry1*, and *zic5* had expression that was predominantly distal, whereas *dner* and *lhx9* had more graded distal to proximal expression and *lmo1* and *msx2*, which both encode transcription factors, were least expressed in the medial region (Figure 7).

3 | CONCLUSIONS

Our analysis of gene expression across the proximal to distal axis of a stage 51 tadpole hindlimb bud provides an unbiased overview of the genes and mechanisms that underlie the patterning of the *Xenopus* limb bud at this critical stage of its development. Stage 51 was chosen based on our previous work proposing a transient, limb bud-autonomous, proximodistal RA gradient.[13] We show that the distal segment, which incorporates the cryptic AER, is the most transcriptionally distinct, and describe the novel expression of a calpain encoding gene, *capn8.3.L* in the flanking regions of the AER. We also identify and describe expression of three further genes previously unlinked to limb development, tightly focused in either the proximal (*tnn.L*, *gata5.L* or distal mesenchymal *zic5*) region of developing *Xenopus* limbs. Gene ontology (GO) analysis of genes expressed differentially between proximal and distal segments provided support for differential cell adhesion, proliferation, Wnt and Fgf signaling as well as RA signaling, although confirmation of these results is beyond the scope of this study. There was no clear pattern to Wnt or Fgf pathway components, with agonists and antagonists for both pathways found both proximally and distally, suggesting regulation of these pathways is complex and nuanced. In contrast, we saw clear evidence for RA signaling. All genes associated with RA receptor signaling were proximal, and all the genes identified as downregulated by RA in a previous study of axolotl limb regeneration[18] were distally expressed in *Xenopus* early hindlimbs. This suggests RA signaling is limited to proximal cells and that RA is actively cleared from distal limb buds. Our findings show support for the model of positional identity conferred by proximal RA and distal Fgf signals in early limb buds proposed by others.[5,6]

4 | EXPERIMENTAL PROCEDURES

4.1 | Animal procedures

All animal procedures were approved by University of Otago's Animal Ethics Committee as AEC56/12. *Xenopus laevis* adult females were injected with 500 U HCG per 75 g bodyweight, into the dorsal lymph sac, to induce egg laying. Eggs were fertilized in vitro using fresh testis preparations and jelly removed with 2% cysteine HCl. From stage 47, tadpoles were fed a suspension of spirulina powder and housed in tanks in a recirculating aquarium.

4.2 | Sample preparation

Stage 51 hindlimb buds were dissected into distal, medial and proximal thirds, each with a length of approximately 200 μM, using Vannas iridectomy scissors. To do this, six tadpoles at a time were anaesthetized with 1/4000 v/v MS222 (tricaine) in 0.1 × MMR (Marc's modified Ringers: 10 mM NaCl, 0.2 mM KCl, 0.1 mM $MgSO_4 \cdot 6H_2O$, 0.2 mM

$CaCl_2$, 0.5 mM HEPES, 10 μM EDTA, pH 7.8). The tadpoles were placed onto damp Whatman paper and the distal third of the hindlimb cut off and placed in 1.5 mL sterile Eppendorf tube cap containing 50 μL of lysis buffer, using sharpened Dumont #5 forceps. When all six distal samples had been collected the cap was placed on a tube containing lysis buffer, spun briefly to pellet the tissue, and placed on dry ice. The process was then repeated for medial sections, and finally for proximal sections by detaching the remaining limb tissue from the body wall cleanly. The tadpoles were then rotated onto the other side and the process repeated with fresh caps. The samples for each region were combined by spinning the new caps with the original tubes. Two different sibships of tadpoles were used, and separately prepared "red" and "black" biological replicates from these were each comprised 30 pooled limb slices per sample.

Distal, medial and proximal samples for each replicate were homogenized with an OMNI TH handheld 5 mm tip probe in 400 μL lysis buffer (Qiagen) for 20 s. RNA was extracted using a Qiagen RNeasy mini kit and on-column DNAse I according to the manufacturer's instructions.

4.3 | Transcriptome sequencing, processing, read mapping, and quantification

Illumina TruSeq RNA Sample Prep Kit was used with 1 μg of each total RNA for the construction of sequencing libraries using standard Illumina protocols. Paired-end sequencing reads were generated by Illumina HiSeq at the Otago Genomics Facility, and data provided as FastQ files. Raw data have been deposited in NCBI Gene expression omnibus (GEO) as GSE179158. Illumina adapter sequences were trimmed from reads and low-quality quality sequences were removed using trimmomatic (version 0.39).[74] HISAT2 (version 2.2.1)[75] was used to align reads for each sample. A HISAT2 index was built from the *X. laevis* transcriptome, genome, and gene models from Xenbase (version 9.2)[76] using the "hisat2--build" command. Samples were aligned using the "hisat2" command, converted to BAM files and sorted using samtools (version 1.10).[77] Sorted files were quantified using the featureCounts (version 2.0.1)[78] which returned a combined quantification file for all samples.

4.4 | Differential expression

The combined quantification file from featureCounts was loaded into R using read. table. The table was made into a DESeq object using the DESeq2[79] command "DESeqDataSetFromMatrix" (options: colData = data. frame(position = factor[position]), design = ~position), where position identified what portion of the limb bud a sample came from. The resulting DESeq object was filtered for transcripts with low counts (counts ≥ 10). The counts table output was made to be a DESeq object with DESeq2's command "DESeqDataSetFromTximport" (options: colData = samples, design = ~position). This DESeq object was also filtered for transcripts with low counts (counts ≥ 10).

Differential expression analysis was performed with the DESeq2 package. Conditions (proximal, medial, and distal segments of limb) were compared using DESeq2's Wald test. The command "DESeq" was used for this with default options. Differential analysis results were filtered for an adjusted p-value < .05, and log2 fold change ±1. Full data can be found in the Appendix S1.

4.5 | Hierarchical read clustering and volcano plot

For each limb segment, the normalized counts from replicates were averaged, and the resulting matrix clustered using the package "ComplexHeatmap"[80] using the command "Heatmap, option: row_km = 7". Rows were clustered using Pearson distance. A full list of genes in each cluster can be found in the Appendix S1. Volcano plots were made using VolcaNoseR.[81]

4.6 | In situ hybridization

Gata5.L, *irx5.L*, *tnn.L*, *sall1.S*, *zic5.S*, *capn8.3.L*, and *dkk1.S* were amplified from reverse transcribed limb bud cDNA and blunt cloned into the EcoRV site of pBSIIKS+. Primers can be found in Table 1. *Fgf8* probe was previously described[82] with modifications for limb buds from McEwan et al.[13] Images were captured using a Leica FluoIII microscope using Leica LS software, with embryos submerged in PBSA on a 2% noble agar lined petri dish and LED lighting. Adobe photoshop CC 2019 was used to assemble figures.

4.7 | GO analysis

GO analysis was performed on significantly differently expressed genes for the proximal versus distal contrast, with a cut-off of log2 ±1.5. The clusterProfiler package[83] and the *X. laevis* genome-wide annotation database[84]

TABLE 1 Primers used to amplify cDNA for in vitro transcription, to generate in situ hybridization probes

	Forward primer	Reverse primer	Size (bp)
Tnn1.L	CAAGGCTTTAGTGGGCCAGA	TCTTCAGTGCTGCCATCAGG	1451
Gata5.L	CAATGGGCCCTTGCAGTTAT	CTTCTGTTCCCCAGTGAGGT	2095
Irx5.L	CTTTGAAGGCGTGGCTTAAC	TCTCTGCCAAGGACCAGAGT	1674
Sall1.S	GCCTGGAAGTCATGAGCAGA	GCTGGGACAAATGGGAACTC	1010
Zic5.S	CGGGATGACGTACTTCGTTT	CACGCCTCTCCTCTTCCATA	1074
Capn8.3.L	CTGGTGCCTGACCCAGTATT	CACATCATGGCGGTACAAAG	2411
Dkk1.S	TCATCCTGCCATTGTGGTTA	GTTCAGGGAAGACCAGAGCA	1297

were used for this. Prior to analysis, gene names were annotated with Entrez IDs using the "GenePageLaevisEntrezGeneUnigeneMapping.txt" file from Xenbase. The "enrichGO" command (options: OrgDb = org.Xl.eg.db, ont = "BP", readable = TRUE) provided enrichment analysis for the genes contained in the proximal versus distal set. All GO levels were included, and 36 terms were significantly over-represented ($P_{Adj} < .05$). Full data for GO can be found in the Appendix S1.

4.8 | Analysis of retinoic acid-regulated genes

Supplemental data from Nguyen et al[18] that identified genes upregualted and downregulated in axolotl limb regeneration supplemental table was manually cross-referenced with DE genes in this study. Genes that did not map to one of the seven clusters, or that had fewer than 100 reads across all samples were eliminated. Read counts of genes both differentially expressed across the proximodistal axis of the *Xenopus* limb bud and regulated by RA in axolotls were plotted for proximal, medial and distal using ggplot2[85] in R and were grouped according to cluster.

AUTHOR CONTRIBUTIONS

Daniel T. Hudson: Data curation (lead); formal analysis (equal); methodology (equal); visualization (equal); writing – original draft (supporting). **Jessica S. Bromell:** Investigation (equal). **Robert C. Day:** Formal analysis (equal); investigation (equal); methodology (supporting); writing – review and editing (supporting). **Tyler McInnes:** Formal analysis (supporting). **Joanna M. Ward:** Investigation (equal); visualization (equal). **Caroline W. Beck:** Conceptualization (lead); formal analysis (supporting); investigation (supporting); methodology (lead); supervision (lead); validation (lead); visualization (lead); writing – original draft (lead); writing – review and editing (lead).

ACKNOWLEDGEMENTS

This work was supported by a University of Otago Research grant to Caroline W. Beck and by the Department of Zoology. We are grateful for the excellent support and maintenance of our *Xenopus* colony provided by Nikita Woodhead. Sequencing was carried out at the Otago Genomics Facility. Open access publishing facilitated by University of Otago, as part of the Wiley - University of Otago agreement via the Council of Australian University Librarians.

DATA AVAILABILITY STATEMENT

Raw RNA-Seq fastq files, the HISAT2/featureCounts table, and a file of significant differential expression is available at NCBI GEO with accession GSE179158. Read counts, differential expression, a list of genes in each cluster, and gene ontology terms can be found in the Supporting Information.

ORCID

Caroline W. Beck https://orcid.org/0000-0001-6489-7425

REFERENCES

1. McQueen C, Towers M. Establishing the pattern of the vertebrate limb. *Development*. 2020;147(17):dev177956. doi:10.1242/dev.177956
2. Pearse RV 2nd, Scherz PJ, Campbell JK, Tabin CJ. A cellular lineage analysis of the chick limb bud. *Dev Biol*. 2007;310(2):388-400. doi:10.1016/j.ydbio.2007.08.002
3. Saunders JW Jr. The proximo-distal sequence of origin of the parts of the chick wing and the role of the ectoderm. *J Exp Zool*. 1948;108(3):363-403. doi:10.1002/jez.1401080304
4. Summerbell D, Lewis JH, Wolpert L. Positional information in chick limb morphogenesis. *Nature*. 1973;244(5417):492-496. doi:10.1038/244492a0
5. Mercader N, Leonardo E, Piedra ME, Martinez AC, Ros MA, Torres M. Opposing RA and FGF signals control proximodistal vertebrate limb development through regulation of Meis genes. *Development*. 2000;127(18):3961-3970.
6. Saiz-Lopez P, Chinnaiya K, Campa VM, Delgado I, Ros MA, Towers M. An intrinsic timer specifies distal structures of the

vertebrate limb. *Nat Commun*. 2015;6:8108. doi:10.1038/ncomms9108
7. Keenan SR, Beck CW. Xenopus limb bud morphogenesis. *Dev Dyn*. 2016;245(3):233-243. doi:10.1002/dvdy.24351
8. Tschumi PA. The growth of the hindlimb bud of Xenopus laevis and its dependence upon the epidermis. *J Anat*. 1957;91(2):149-173.
9. Christen B, Slack JM. FGF-8 is associated with anteroposterior patterning and limb regeneration in Xenopus. *Dev Biol*. 1997;192(2):455-466. doi:10.1006/dbio.1997.8732
10. Endo T, Tamura K, Ide H. Analysis of gene expressions during Xenopus forelimb regeneration. *Dev Biol*. 2000;220(2):296-306. doi:10.1006/dbio.2000.9641
11. Jones TE, Day RC, Beck CW. Attenuation of bone morphogenetic protein signaling during amphibian limb development results in the generation of stage-specific defects. *J Anat*. 2013;223(5):474-488. doi:10.1111/joa.12098
12. Wang YH, Beck CW. Distal expression of sprouty (spry) genes during *Xenopus laevis* limb development and regeneration. *Gene Expr Patterns*. 2014;15(1):61-66. doi:10.1016/j.gep.2014.04.004
13. McEwan J, Lynch J, Beck CW. Expression of key retinoic acid modulating genes suggests active regulation during development and regeneration of the amphibian limb. *Dev Dyn*. 2011;240(5):1259-1270. doi:10.1002/dvdy.22555
14. Tarin D, Sturdee AP. Early limb development of *Xenopus laevis*. *J Embryol Exp Morphol*. 1971;26(2):169-179.
15. Miura S, Hanaoka K, Togashi S. Skeletogenesis in *Xenopus tropicalis*: characteristic bone development in an anuran amphibian. *Bone*. 2008;43(5):901-909. doi:10.1016/j.bone.2008.07.005
16. Satoh A, Suzuki M, Amano T, Tamura K, Ide H. Joint development in *Xenopus laevis* and induction of segmentations in regenerating froglet limb (spike). *Dev Dyn*. 2005;233(4):1444-1453. doi:10.1002/dvdy.20484
17. Martin BL, Harland RM. A novel role for lbx1 in *Xenopus* hypaxial myogenesis. *Development*. 2006;133(2):195-208. doi:10.1242/dev.02183
18. Nguyen M, Singhal P, Piet JW, et al. Retinoic acid receptor regulation of epimorphic and homeostatic regeneration in the axolotl. *Development*. 2017;144(4):601-611. doi:10.1242/dev.139873
19. Delgado I, Lopez-Delgado AC, Rosello-Diez A, et al. Proximodistal positional information encoded by an Fgf-regulated gradient of homeodomain transcription factors in the vertebrate limb. *Sci Adv*. 2020;6(23):eaaz0742. doi:10.1126/sciadv.aaz0742
20. Haworth KE, Kotecha S, Mohun TJ, Latinkic BV. GATA4 and GATA5 are essential for heart and liver development in *Xenopus* embryos. *BMC Dev Biol*. 2008;8:74. doi:10.1186/1471-213X-8-74
21. Kozhemyakina E, Ionescu A, Lassar AB. GATA6 is a crucial regulator of Shh in the limb bud. *PLoS Genet*. 2014;10(1):e1004072. doi:10.1371/journal.pgen.1004072
22. Hayashi S, Akiyama R, Wong J, Tahara N, Kawakami H, Kawakami Y. Gata6-dependent GLI3 repressor function is essential in anterior limb progenitor cells for proper limb development. *PLoS Genet*. 2016;12(6):e1006138. doi:10.1371/journal.pgen.1006138
23. Jiang Y, Evans T. The *Xenopus* GATA-4/5/6 genes are associated with cardiac specification and can regulate cardiac-specific transcription during embryogenesis. *Dev Biol*. 1996;174(2):258-270. doi:10.1006/dbio.1996.0071
24. Rodriguez-Seguel E, Alarcon P, Gomez-Skarmeta JL. The Xenopus Irx genes are essential for neural patterning and define the border between prethalamus and thalamus through mutual antagonism with the anterior repressors Fezf and Arx. *Dev Biol*. 2009;329(2):258-268. doi:10.1016/j.ydbio.2009.02.028
25. Session AM, Uno Y, Kwon T, et al. Genome evolution in the allotetraploid frog *Xenopus laevis*. *Nature*. 2016;538(7625):336-343. doi:10.1038/nature19840
26. Li D, Sakuma R, Vakili NA, et al. Formation of proximal and anterior limb skeleton requires early function of Irx3 and Irx5 and is negatively regulated by Shh signaling. *Dev Cell*. 2014;29(2):233-240. doi:10.1016/j.devcel.2014.03.001
27. Bonnard C, Strobl AC, Shboul M, et al. Mutations in IRX5 impair craniofacial development and germ cell migration via SDF1. *Nat Genet*. 2012;44(6):709-713. doi:10.1038/ng.2259
28. Weber P, Montag D, Schachner M, Bernhardt RR. Zebrafish tenascin-W, a new member of the tenascin family. *J Neurobiol*. 1998;35(1):1-16.
29. Tucker RP, Degen M. The expression and possible functions of tenascin-W during development and disease. *Front Cell Dev Biol*. 2019;7:53. doi:10.3389/fcell.2019.00053
30. Ahn K, Mishina Y, Hanks MC, Behringer RR, Crenshaw EB 3rd. BMPR-IA signaling is required for the formation of the apical ectodermal ridge and dorsal–ventral patterning of the limb. *Development*. 2001;128(22):4449-4461. doi:10.1242/dev.128.22.4449
31. Bell SM, Schreiner CM, Waclaw RR, Campbell K, Potter SS, Scott WJ. Sp8 is crucial for limb outgrowth and neuropore closure. *Proc Natl Acad Sci USA*. 2003;100(21):12195-12200. doi:10.1073/pnas.2134310100
32. Bulfone A, Kim HJ, Puelles L, Porteus MH, Grippo JF, Rubenstein JL. The mouse Dlx-2 (Tes-1) gene is expressed in spatially restricted domains of the forebrain, face and limbs in midgestation mouse embryos. *Mech Dev*. 1993;40(3):129-140. doi:10.1016/0925-4773(93)90071-5
33. Gorivodsky M, Lonai P. Novel roles of Fgfr2 in AER differentiation and positioning of the dorsoventral limb interface. *Development*. 2003;130(22):5471-5479. doi:10.1242/dev.00795
34. Spinozzi S, Albini S, Best H, Richard I. Calpains for dummies: what you need to know about the calpain family. *Biochim Biophys Acta Proteins Proteom*. 2021;1869(5):140616. doi:10.1016/j.bbapap.2021.140616
35. Luo T, Zhang Y, Khadka D, Rangarajan J, Cho KW, Sargent TD. Regulatory targets for transcription factor AP2 in Xenopus embryos. *Dev Growth Differ*. 2005;47(6):403-413. doi:10.1111/j.1440-169X.2005.00809.x
36. Macqueen DJ, Wilcox AH. Characterization of the definitive classical calpain family of vertebrates using phylogenetic, evolutionary and expression analyses. *Open Biol*. 2014;4:130219. doi:10.1098/rsob.130219
37. Bowes JB, Snyder KA, Segerdell E, et al. Xenbase: a Xenopus biology and genomics resource. *Nucleic Acids Res*. 2008;36-(Database issue):D761-D767. doi:10.1093/nar/gkm826
38. Glinka A, Wu W, Delius H, Monaghan AP, Blumenstock C, Niehrs C. Dickkopf-1 is a member of a new family of secreted proteins and functions in head induction. *Nature*. 1998;391(6665):357-362. doi:10.1038/34848

39. Grotewold L, Theil T, Ruther U. Expression pattern of Dkk-1 during mouse limb development. *Mech Dev*. 1999;89(1–2):151-153. doi:10.1016/s0925-4773(99)00194-x
40. Monaghan AP, Kioschis P, Wu W, et al. Dickkopf genes are coordinately expressed in mesodermal lineages. *Mech Dev*. 1999;87(1–2):45-56. doi:10.1016/s0925-4773(99)00138-0
41. Mukhopadhyay M, Shtrom S, Rodriguez-Esteban C, et al. Dickkopf1 is required for embryonic head induction and limb morphogenesis in the mouse. *Dev Cell*. 2001;1(3):423-434. doi:10.1016/s1534-5807(01)00041-7
42. Grotewold L, Ruther U. The Wnt antagonist Dickkopf-1 is regulated by bmp signaling and c-Jun and modulates programmed cell death. *EMBO J*. 2002;21(5):966-975. doi:10.1093/emboj/21.5.966
43. Lieven O, Knobloch J, Ruther U. The regulation of Dkk1 expression during embryonic development. *Dev Biol*. 2010;340(2):256-268. doi:10.1016/j.ydbio.2010.01.037
44. Lewandoski M, Sun X, Martin GR. Fgf8 signalling from the AER is essential for normal limb development. *Nat Genet*. 2000;26(4):460-463. doi:10.1038/82609
45. Moon AM, Capecchi MR. Fgf8 is required for outgrowth and patterning of the limbs. *Nat Genet*. 2000;26(4):455-459. doi:10.1038/82601
46. Christen B, Beck CW, Lombardo A, Slack JM. Regeneration-specific expression pattern of three posterior Hox genes. *Dev Dyn*. 2003;226(2):349-355. doi:10.1002/dvdy.10231
47. Townes PL, Brocks ER. Hereditary syndrome of imperforate anus with hand, foot, and ear anomalies. *J Pediatr*. 1972;81(2):321-326. doi:10.1016/s0022-3476(72)80302-0
48. Buck A, Kispert A, Kohlhase J. Embryonic expression of the murine homologue of SALL1, the gene mutated in Townes–Brocks syndrome. *Mech Dev*. 2001;104(1–2):143-146. doi:10.1016/s0925-4773(01)00364-1
49. Farrell ER, Munsterberg AE. csal1 is controlled by a combination of FGF and Wnt signals in developing limb buds. *Dev Biol*. 2000;225(2):447-458. doi:10.1006/dbio.2000.9852
50. Neff AW, King MW, Mescher AL. Dedifferentiation and the role of sall4 in reprogramming and patterning during amphibian limb regeneration. *Dev Dyn*. 2011;240(5):979-989. doi:10.1002/dvdy.22554
51. Aruga J, Kamiya A, Takahashi H, et al. A wide-range phylogenetic analysis of Zic proteins: implications for correlations between protein structure conservation and body plan complexity. *Genomics*. 2006;87(6):783-792. doi:10.1016/j.ygeno.2006.02.011
52. Houtmeyers R, Souopgui J, Tejpar S, Arkell R. The ZIC gene family encodes multi-functional proteins essential for patterning and morphogenesis. *Cell Mol Life Sci*. 2013;70(20):3791-3811. doi:10.1007/s00018-013-1285-5
53. Pan H, Gustafsson MK, Aruga J, Tiedken JJ, Chen JC, Emerson CP Jr. A role for Zic1 and Zic2 in Myf5 regulation and somite myogenesis. *Dev Biol*. 2011;351(1):120-127. doi:10.1016/j.ydbio.2010.12.037
54. Wada N. Spatiotemporal changes in cell adhesiveness during vertebrate limb morphogenesis. *Dev Dyn*. 2011;240(5):969-978. doi:10.1002/dvdy.22552
55. da Silva SM, Gates PB, Brockes JP. The newt ortholog of CD59 is implicated in proximodistal identity during amphibian limb regeneration. *Dev Cell*. 2002;3(4):547-555. doi:10.1016/s1534-5807(02)00288-5
56. Whited JL, Lehoczky JA, Austin CA, Tabin CJ. Dynamic expression of two thrombospondins during axolotl limb regeneration. *Dev Dyn*. 2011;240(5):1249-1258. doi:10.1002/dvdy.22548
57. Pearl EJ, Barker D, Day RC, Beck CW. Identification of genes associated with regenerative success of *Xenopus laevis* hindlimbs. *BMC Dev Biol*. 2008;8:66. doi:10.1186/1471-213X-8-66
58. Bose K, Nischt R, Page A, Bader BL, Paulsson M, Smyth N. Loss of nidogen-1 and -2 results in syndactyly and changes in limb development. *J Biol Chem*. 2006;281(51):39620-39629. doi:10.1074/jbc.M607886200
59. Riddle RD, Ensini M, Nelson C, Tsuchida T, Jessell TM, Tabin C. Induction of the LIM homeobox gene Lmx1 by WNT7a establishes dorsoventral pattern in the vertebrate limb. *Cell*. 1995;83(4):631-640. doi:10.1016/0092-8674(95)90103-5
60. Wu W, Glinka A, Delius H, Niehrs C. Mutual antagonism between dickkopf1 and dickkopf2 regulates Wnt/beta-catenin signalling. *Curr Biol*. 2000;10(24):1611-1614. doi:10.1016/s0960-9822(00)00868-x
61. Pinho S, Niehrs C. Dkk3 is required for TGF-beta signaling during Xenopus mesoderm induction. *Differentiation*. 2007;75(10):957-967. doi:10.1111/j.1432-0436.2007.00185.x
62. Dealy CN, Roth A, Ferrari D, Brown AM, Kosher RA. Wnt-5a and Wnt-7a are expressed in the developing chick limb bud in a manner suggesting roles in pattern formation along the proximodistal and dorsoventral axes. *Mech Dev*. 1993;43(2-3):175-186. doi:10.1016/0925-4773(93)90034-u
63. Parr BA, Shea MJ, Vassileva G, McMahon AP. Mouse Wnt genes exhibit discrete domains of expression in the early embryonic CNS and limb buds. *Development*. 1993;119(1):247-261. doi:10.1242/dev.119.1.247
64. Lovely AM, Duerr TJ, Qiu Q, Galvan S, Voss SR, Monaghan JR. Wnt signaling coordinates the expression of limb patterning genes during axolotl forelimb development and regeneration. *Front Cell Dev Biol*. 2022;10:814250. doi:10.3389/fcell.2022.814250
65. Gao B, Ajima R, Yang W, et al. Coordinated directional outgrowth and pattern formation by integration of Wnt5a and Fgf signaling in planar cell polarity. *Development*. 2018;145(8):dev163824. doi:10.1242/dev.163824
66. Saad K, Otto A, Theis S, et al. Detailed expression profile of all six Glypicans and their modifying enzyme notum during chick embryogenesis and their role in dorsal–ventral patterning of the neural tube. *Gene*. 2017;609:38-51. doi:10.1016/j.gene.2017.01.032
67. Nathan E, Tzahor E. sFRPs: a declaration of (Wnt) independence. *Nat Cell Biol*. 2009;11(1):13. doi:10.1038/ncb0109-13
68. Martin GR. The roles of FGFs in the early development of vertebrate limbs. *Genes Dev*. 1998;12(11):1571-1586. doi:10.1101/gad.12.11.1571
69. Wang YH, Beck C. Distinct patterns of endosulfatase gene expression during *Xenopus laevis* limb development and regeneration. *Regeneration (Oxf)*. 2015;2(1):19-25. doi:10.1002/reg2.27
70. Tamura K, Yokouchi Y, Kuroiwa A, Ide H. Retinoic acid changes the proximodistal developmental competence and

affinity of distal cells in the developing chick limb bud. *Dev Biol*. 1997;188(2):224-234. doi:10.1006/dbio.1997.8627
71. Maden M. Vitamin a and pattern formation in the regenerating limb. *Nature*. 1982;295(5851):672-675. doi:10.1038/295672a0
72. Monaghan JR, Maden M. Visualization of retinoic acid signaling in transgenic axolotls during limb development and regeneration. *Dev Biol*. 2012;368(1):63-75. doi:10.1016/j.ydbio.2012.05.015
73. Cunningham TJ, Duester G. Mechanisms of retinoic acid signalling and its roles in organ and limb development. *Nat Rev Mol Cell Biol*. 2015;16(2):110-123. doi:10.1038/nrm3932
74. Bolger AM, Lohse M, Usadel B. Trimmomatic: a flexible trimmer for Illumina sequence data. *Bioinformatics*. 2014;30(15):2114-2120. doi:10.1093/bioinformatics/btu170
75. Kim D, Langmead B, Salzberg SL. HISAT: a fast spliced aligner with low memory requirements. *Nat Methods*. 2015;12(4):357-360. doi:10.1038/nmeth.3317
76. Karimi K, Fortriede JD, Lotay VS, et al. Xenbase: a genomic, epigenomic and transcriptomic model organism database. *Nucleic Acids Res*. 2018;46(D1):D861-D868. doi:10.1093/nar/gkx936
77. Li H, Handsaker B, Wysoker A, et al. The sequence alignment/map format and SAMtools. *Bioinformatics*. 2009;25(16):2078-2079. doi:10.1093/bioinformatics/btp352
78. Liao Y, Smyth GK, Shi W. featureCounts: an efficient general purpose program for assigning sequence reads to genomic features. *Bioinformatics*. 2014;30(7):923-930. doi:10.1093/bioinformatics/btt656
79. Love MI, Huber W, Anders S. Moderated estimation of fold change and dispersion for RNA-seq data with DESeq2. *Genome Biol*. 2014;15(12):550. doi:10.1186/s13059-014-0550-8
80. Gu Z, Eils R, Schlesner M. Complex heatmaps reveal patterns and correlations in multidimensional genomic data. *Bioinformatics*. 2016;32(18):2847-2849. doi:10.1093/bioinformatics/btw313
81. Goedhart J, Luijsterburg MS. VolcaNoseR is a web app for creating, exploring, labeling and sharing volcano plots. *Sci Rep*. 2020;10(1):20560. doi:10.1038/s41598-020-76603-3
82. Pownall ME, Tucker AS, Slack JM, Isaacs HV. eFGF, Xcad3 and Hox genes form a molecular pathway that establishes the anteroposterior axis in Xenopus. *Development*. 1996;122(12):3881-3892. doi:10.1242/dev.122.12.3881
83. Yu G, Wang LG, Han Y, He QY. clusterProfiler: an R package for comparing biological themes among gene clusters. *Omics*. 2012;16(5):284-287. doi:10.1089/omi.2011.0118
84. Carlson M. org.Xl.eg.db: Genome wide annotation for Xenopus. R package version 3.8.2; 2019.
85. Wickham H. *ggplot2: Elegant graphics for data analysis*. New York: Springer-Verlag; 2016.
86. Oliveros JC. *Venny. An interactive tool for comparing lists with Venn's diagrams*. Wuhan, China: Scientific Research Publishing; 2007-2015. https://bioinfogp.cnb.csic.es/tools/venny/index.html.

SUPPORTING INFORMATION

Additional supporting information can be found online in the Supporting Information section at the end of this article.

How to cite this article: Hudson DT, Bromell JS, Day RC, McInnes T, Ward JM, Beck CW. Gene expression analysis of the *Xenopus laevis* early limb bud proximodistal axis. *Developmental Dynamics*. 2022;251(11):1880-1896. doi:10.1002/dvdy.517